Optimal feedback control for route tracking with a bounded–curvature vehicle

Philippe Souères
LAAS - CNRS
7 Av. du colonel Roche
31077 Toulouse Cedex 4
FRANCE
soueres@laas.fr

Andrea Balluchi
PARADES E.E.I.G
Via San Pantaleo, 66
00186 Roma
ITALY
balluchi@parades.rm.cnr.it

Antonio Bicchi
Centro Interdipartimentale
di Ricerca "Enrico Piaggio"
Univ. di Pisa
56100 Pisa, ITALY
bicchi@ing.unipi.it

Abstract

The problem of driving a vehicle along a given path is considered. The vehicle is supposed to move forward only, with a given velocity profile, and to have bounds on its turning radius. Such a model, also known as "Dubins' vehicle", is relevant to the kinematics of road vehicles as well as aircraft cruising at constant altitude, or sea vessels. We consider the optimal control problem consisting of minimizing the length travelled by the vehicle starting from a generic configuration to connect to a specified route. A feedback law is proposed, such that straight routes can be approached optimally, while the system is asymptotically stabilized. Experimental results are reported showing real–time feasibility of the proposed approach.

keywords: Optimal control, regular synthesis, route tracking, nonholonomic vehicles.

1 Introduction

In this paper, we consider the problem of driving a vehicle along a given route. We consider the so–called Dubins' model for the vehicle, whose motion is restricted to a plane, and is subject to a nonholonomic constraint on the trajectory (no velocity allowed in the direction perpendicular to the main axis of the vehicle), to the specification of a unidirectional velocity profile (only forward motion at given speed profile allowed), and to a limitation on the curvature of the trajectory (bounded yaw rate, or steering radius) [10].

Such model ignores the vehicle dynamics, and is therefore a rather idealized model for practical vehicles. However, it explicitly takes into account inherent limitations of automobiles along highways and aircraft cruising at constant altitude, thus providing a complete model of the kinematics involved, and a reference framework for extending results to more complex models. Constraints on the direction of motion of the vehicle, and on its curvature, are reflected in input bounds that have not been previously considered in the route tracking problem (see discussion below).

We propose an hybrid feedback control law for Dubins' model for tracking rectilinear routes. This controller locally stabilizes the vehicle on the route, and guarantees global convergence in finite–time. It is also shown to achieve optimal (in the shortest-length sense) connecting paths to the route. The study of convergence and optimality is done using Pontryagin's maximum principle (henceforth PMP, [15]) completed with global geometric arguments. Afterwards, we prove that the optimality of paths can be confirmed by applying sufficient optimality conditions provided by a regular synthesis theorem [14] [3]. Stability is discussed in a hybrid control framework.

The paper is organized as follows. Related works are presented in section section 1.1. In section 2 we formalize and provide a complete solution to the optimal tracking problem for rectilinear paths. In section 3 we synthesize a feedback controller that implements optimal trajectories, formalize it as an hybrid control system, and prove its global asymptotic stability. Finally, in section 4 experimental results are presented demonstrating the practical feasibility of the proposed control laws.

1.1 Related work

The literature on planning and control techniques for nonholonomic vehicles has grown extensive in the recent few years, providing results among which a few have a direct bearing to the work reported in this paper. In particular, it was shown that the kinematic model of a vehicle that can drive both forward and backward with bounded curvature (but allowing cusps in the path, such as e.g. in the case of an automobile in a parking maneuver), is locally controllable. A vehicle that can only move forward and is subject to curvature bounds (such as the model under consideration here) is still controllable, although not small time locally controllable. For this latter type of vehicle, Dubins [10] studied the shortest paths joining two arbitrary configurations. He proved that optimal paths can be built with at most three pieces of either type "C" (arcs of circle with minimal radius R), or type "S" (straight line segments). Furthermore, optimal paths necessarily belong to the following sufficient family made of two path types only,

$$\{C_a C_b C_e \ , \ C_u S_d C_v\} \tag{1}$$

where the subscripts, indicating the length of each piece, are restricted respectively to

$$b \in (\pi R, 2\pi R); \ \ a, e \in [0, b], \ \ u, v \in [0, 2\pi R), \ \ d \geq 0 \tag{2}$$

Reeds and Shepp [16] extended Dubins' results to a vehicle that can reverse its motion. Later, [24] and [4], gave new proofs of Dubins' result and Reeds and Shepp's result by using optimal control theory. Finally, on the basis of these works, the complete synthesis of optimal paths was constructed in [6] for Dubin's problem, and in [23] for Reeds and Shepp's problem, providing a complete solution of the open–loop point-to-point planning problem.

On the other hand, the feedback stabilization problem is particularly challenging for nonholonomic vehicles [5]. Stabilization to a configuration has been widely studied, and partially solved via non–smooth (see e.g. [22, 1, 2, 11]), time–varying ([18, 7, 17]), and dynamic extension feedback algorithms

(cf. e.g. [8, 9]). Trajectory or route tracking control is simpler in principle for nonholonomic systems.[1] Previous work on trajectory tracking and route following includes [26, 21, 19]. The paper of Samson [18] has a thorough treatment of systems in chained form (hence, of more general vehicles than are considered here), and solves the problems of route following, trajectory tracking, and point stabilization in a uniform, elegant way.

As opposite to work in route planning, most literature on vehicle stabilization does not consider curvature bounds in the vehicle model. On the other hand, as already noted, most real–world vehicles have limited turning radii. In this paper, we attack and give an optimal solution to the route following problem under path curvature bounds.

2 Shortest paths to join straight routes

Let the configuration of the vehicle be described as $X = (M, \theta) \in \mathbb{R}^2 \times S^1$, with $M := (x, y)$ coordinates of a reference point in the vehicle and θ is the angle made by the vehicle direction, with respect to some fixed reference frame in the plane. The kinematics of the vehicle is described by

$$\begin{cases} \dot{x} = v\cos\theta \\ \dot{y} = v\sin\theta \\ \dot{\theta} = \omega \end{cases} \tag{3}$$

where v is the forward velocity of the vehicle, and ω is its turning (yawing) rate. The vehicle is thus constrained to move tangentially to its main axis, with a given linear velocity $v(t) > 0$. Without loss of generality, up to a time–axis rescaling (cf. e.g. [17]), we assume that $\dot{v}(t) = 0$, $v(t) \equiv V$. The turning radius of the vehicle is lower bounded by a constant value $R > 0$, which results in an upper bound on the vehicle's angular velocity ω as

$$|\omega| < \frac{V}{R}. \tag{4}$$

Let $\mathcal{T}$ be a rectilinear route in the plane, with a prescribed direction of motion determined by the angle $\alpha \in [-\pi, \pi]$ with respect to the x–axis (see figure 9). We consider the optimal control problem:

$$\text{Minimize } J = \int_0^T \sqrt{\dot{x}^2 + \dot{y}^2}\,dt = VT, \tag{5}$$

subject to (3) and (4), with $X(0) = (M_0, \theta_0)$ and such that, at the unspecified terminal time T, $M(T) \in \mathcal{T}$ and $\theta(T) = \alpha$.

The determination of optimal paths is done as follows: In section 2.1 we characterize extremal solutions by applying PMP [15] along the lines of [24], [4], and [23], then in section 2.2 we complete the characterization of optimal paths by using global geometric arguments. From this result we construct a synthesis of optimal paths in section 2.3 which provides a complete solution to the problem. Finally, in section 2.4 we show that our result can be confirmed by applying a theorem which guarantees sufficient optimality conditions from the regularity properties of the synthesis [3], [14].

[1] By "route" or "path" we refer to a curve in the plane where the vehicle moves. The former is preferred to indicate prespecified reference curves. By "trajectory" we mean a path with an associated time law.

2.1 Characterization of extremal arcs

As the linear velocity v is constant, the minimum-length problem is equivalent to a minimum-time problem. The Hamiltonian associated to our problem is

$$\mathcal{H}(\psi, X, \omega) = \psi_1 V \cos\theta + \psi_2 V \sin\theta + \psi_3 \omega, \tag{6}$$

where $\psi = (\psi_1, \psi_2, \psi_3)^T$ is the system costate.

We will consider controls in the class ω of piecewise continuous function on $[0, T]$ taking values in $[-\frac{V}{R}, +\frac{V}{R}]$. Such choice for the admissible controls, motivated by practical applications, may appear to be somewhat restrictive. However this is not the case. In fact, necessary conditions for extremals could be worked out for the much more general class of bounded measurable controls, in exactly the same way as we do below for piecewise continuous controls (see [15]). However, we will show that the class Ω actually contains optimal controls, hence no improvement in cost could be obtained by using bounded measurable controls that are not in Ω.

According to PMP, a necessary condition for the control $\omega^*(t)$ to be optimal is that the adjoint vector $\psi(t)$ is continuous and nonzero, and that there exists a negative constant ψ_0, such that at all times $t \in [0, T]$

$$-\psi_0 = \mathcal{H}(\psi(t), X(t), \omega^*(t)) = \min_{\omega \in \Omega} \mathcal{H}(\psi(t), X(t), \omega(t)), \tag{7}$$

Writing the adjoint equations

$$\dot{\psi}(t) = -\frac{\partial \mathcal{H}}{\partial X}(\psi(t), X(t), \omega^*(t)) \tag{8}$$

we get

$$\frac{\partial \mathcal{H}}{\partial x} = \frac{\partial \mathcal{H}}{\partial y} = 0 \quad \Rightarrow \quad \psi_1 \text{ and } \psi_2 \text{ are constant,}$$

and

$$\frac{\partial \psi_3}{\partial t} = -\frac{\partial \mathcal{H}}{\partial \theta} = V(\psi_1 \sin\theta - \psi_2 \cos\theta) = \psi_1 \dot{y} - \psi_2 \dot{x},$$

which gives

$$\psi_3(t) = \psi_3(0) + \psi_1(y(t) - y(0)) - \psi_2(x(t) - x(0)). \tag{9}$$

From (6), the third costate component $\psi_3(t)$ is the switching function for ω^*. As described in [23], two cases may occur along an optimal path:

1. ω^* is regular, i.e. ψ_3 only vanishes at isolated points of $[0, T]$. In that case, we deduce from (7) that $|\omega| = \frac{V}{R}$ and the sign of ω is opposite to the sign of ψ_3. The path is made of arcs C.

2. ω is singular, i.e. ψ_3 vanishes over a non zero interval $I \subset [0, T]$. From nontriviality of the costate and from (7) we deduce that

$$-\psi_0 = \psi_1 V \cos\theta + \psi_2 V \sin\theta, \quad \forall t \in I. \tag{10}$$

   Hence, $\theta(t)$ keeps constant along I and the resulting motion is a line segment S.

Control switches between two arcs C (points of inflection) or between an arc C and a line segment S, occur when $\psi_3 = 0$. According to (9) the relation $\psi_3(t) = 0$ determines a vertical plane in $\mathbb{R}^2 \times [-2\pi, 2\pi]$,

$$\psi_1 y(t) - \psi_2 x(t) + \psi_3(0) - \psi_1 y(0) + \psi_2 x(0) = 0. \tag{11}$$

Projecting this plane perpendicularly on the plane of the vehicle's motion we obtain a line $\mathcal{D}$ described by (11), a tangent vector of which is given by $(\psi_1, \psi_2)^T$. Hence, the line $\mathcal{D}$ supports all line segments and points of inflection of all optimal paths.

In our optimal control problem, a supplementary transversality condition applies stating that, at the unspecified final time T, $\psi(T) \perp \mathcal{T}$. As $(\cos\alpha, \sin\alpha, 0)^T$ is a vector tangent to $\mathcal{T}$, the transversality condition states:

$$\cos(\alpha)\psi_1(T) + \sin(\alpha)\psi_2(T) = 0. \tag{12}$$

Hence, we have the following:

Lemma 1 *Optimal paths solving problem (5) belong to the Dubins' family (1), and are such that rectilinear segments and points of inflection belong to an unique line $\mathcal{D}$ perpendicular to the target line $\mathcal{T}$.*

On the basis of lemma 1, the family (1), (2) can be further refined using geometric arguments.

2.2 Refinement of the sufficient family

Notation To specify the vehicle's direction of motion, we replace the (C) by (l) for left turn or by (r) for right turn. Each path will be represented by a word belonging to the family $\{lrl, rlr, lsl, rsr, rsl, lsr\}$. Subscripts are used to specify the length of each piece.

Property 1 *In the plane of the vehicle's motion, let Δ be the line of equation $y cos\frac{\theta}{2} + x sin\frac{\theta}{2} = 0$, and M, M' any two points symmetric with respect to Δ. If γ is a path starting from $(O,0)$ and ending at (M,θ), there exists a path γ' isometric to γ, starting from $(O,0)$ and ending at (M',θ). The word for γ' is obtained by writing the word for γ in reverse direction.*

Property 1 is illustrated by figure 1. The proof can be directly deduced from [23], lemma 1, p 676. The problem was stated in terms of ending at $(O,0)$, but the reasoning for our problem is similar[2].

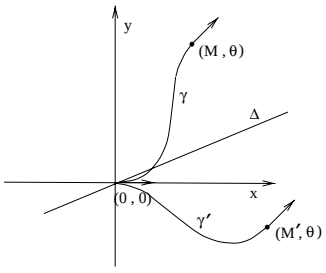

Figure 1: Symmetry in plane of the vehicle's motion

Two isometric paths have then naturally the same length, therefore when they link the same two oriented points they are equivalent for our optimization problem.

[2]In that work Δ was denoted by $\Delta_\theta^\perp$ and the symmetric points here called M and M' were called M and M_3.

Consider now the case that the final orientation of paths is π. In that case the line Δ is identical to the $y-$axis and the directed points (M,π) and (M',π) belong necessarily to the same directed line $\mathcal{T}$, parallel to the x-axis (see figure 2). From property 1 both paths are equivalent for linking $(O,0)$ to $\mathcal{T}$. This result can be stated in a more general way as follows:

Property 2 *If γ is a path starting from (M,θ) and reaching $\mathcal{T}$ with orientation $\alpha = \theta \pm \pi$, there exists an isometric path γ' from (M,θ) to $\mathcal{T}$. The word for γ' is obtained by writing the word for γ in the reverse direction.*

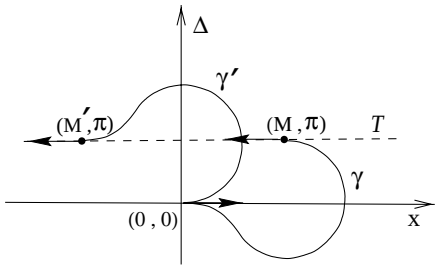

Figure 2: Isometric paths $r_{(\pi R+a)}l_a$ and $l_a r_{(\pi R+a)}$

Property 3 *A path CCC is never optimal for reaching tangentially a directing line.*

Proof: Suppose that a path $l_a r_b l_e$ is optimal for linking a point (M_0,θ) to $\mathcal{T}$ with direction α (same reasoning for path $r_a l_b r_e$). From (2) a necessary condition for such a path to be optimal is that $b > \pi R$. Lemma 1 indicates that both points of inflection belong to a line $\mathcal{D} \perp \mathcal{T}$. It follows that $b = \pi R + 2e$. There exist then necessarily a point M_1 belonging to the middle arc r of the path, whose direction is $\alpha + \pi$. Consider the subpath $\gamma : r_{(\pi R+e)}l_e$ linking $(M_1, \alpha+\pi)$ to $\mathcal{T}$. From property 2 there exists an equivalent path $\gamma' : l_e r_{(\pi R+e)}$ linking also $(M_1,\alpha+\pi)$ to $\mathcal{T}$. The initial path $l_a r_b l_e$ is equivalent to the path $l_a r_e l_e r_{(\pi R+e)}$ obtained by replacing the subpath γ by γ'. As this last path contains three points of inflection which do not belong to a line $\mathcal{D} \perp \mathcal{T}$, it cannot be optimal (see figure 3). The initial path $l_a r_b l_e$, being equivalent to a nonoptimal path, is itself nonoptimal. □

According to (1) and property 3 it suffices to consider paths CSC. Obviously, this path type contains the subtypes CC, C and SC (a path S_d with $d > 0$ is trivially not optimal for reaching tangentially $\mathcal{T}$).

Property 4 *A necessary condition for a path C_a to be optimal is that $a \leq \frac{3\pi}{2}R$*

Proof: If $a = \frac{3\pi}{2}R + \varepsilon$ there exist an equivalent path $C_\varepsilon C_{\pi R} C_{\frac{\pi}{2}R}$ which is not optimal because the line $\mathcal{D}$ containing the two points of inflection is parallel to the target line (see figure 4). □

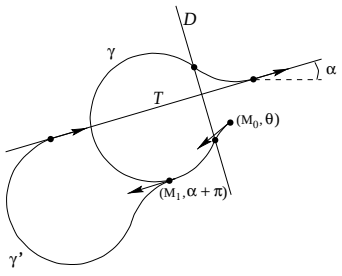

Figure 3: A path $l_a r_b l_e$ equivalent to $l_a r_e l_\varepsilon r_{\pi+e}$

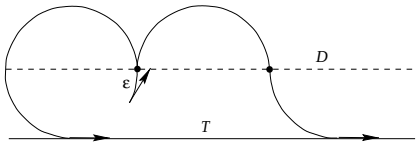

Figure 4: A path $l_{\frac{3\pi}{2}R+\varepsilon}$ equivalent to $l_\varepsilon r_{\pi R} l_{\frac{\pi}{2}R}$

Property 5 *A necessary condition for a path $C_a C_b$ to be optimal is that one of the following two conditions be verified:*

- $b \in [0, \frac{\pi}{2}R]$ *and* $a \in [0, b + \pi R]$,
- $b \in [\pi R, \frac{3\pi}{2}R]$ *and* $a \in [0, b - \pi R]$,

Proof: Consider a path $l_a r_b$ with $\frac{\pi}{2}R < b < \pi R$. The line $\mathcal{D} \perp \mathcal{T}$ containing the point of inflection I, cuts the last arc r at a point N where the control ω does not switch (see figure 5). However, as stated in §2.1, the control must switch each time $\mathcal{D}$ is crossed; therefore, $b \in [0, \frac{\pi}{2}R]$ or $b \in [\pi R, \frac{3\pi}{2}R]$.

- If $b \in [0, \frac{\pi}{2}R]$ and $a = b + \pi R + \varepsilon$, $\varepsilon > 0$, there exists a point $(M, \alpha - \pi)$ on the first arc (α being the direction of $\mathcal{T}$). The subpath $l_{(b+\pi R)} r_b$, linking $(M, \alpha - \pi)$ to $\mathcal{T}$, can be replaced by an equivalent path $r_b l_{(b+\pi R)}$ (see figure 6). The path $l_a r_b$ is then equivalent to a path $l_\varepsilon r_b l_{(b+\pi R)}$ which is not optimal according to property 3. Then, necessarily $a \in [0, b + \pi R]$.

- If $b \in [\pi R, \frac{3\pi}{2}R]$ and $a = b - \pi R + \varepsilon$, there exists a point $(M, \alpha - \pi)$ on the first arc l. Using the same reasoning, we deduce the existence of an equivalent subpath $r_b l_{a-\varepsilon}$ linking $(M, \alpha - \pi)$ to $\mathcal{T}$. The initial path $l_a r_b$ is equivalent to a path $l_\varepsilon r_b l_{a-\varepsilon}$ which is not optimal according to property 3. Then, necessarily $a \in [0, b - \pi R]$.

The same reasoning applies to paths of type $r_a l_b$. □

Property 6 *A necessary condition for a path $C_a S_d C_b$ to be optimal is that the segment S be perpendicular to $\mathcal{T}$, $a \in [0, \pi R]$ and $b = \frac{\pi}{2}R$.*

Proof: ¿From lemma 1 the segment S belongs to $\mathcal{D} \perp \mathcal{T}$. Therefore, necessarily, $b = \frac{\pi R}{2}$ or $b = \frac{3\pi R}{2}$. If $b = \frac{3\pi}{2}R$, the path is equivalent to a path $CSC_{\pi R} C_{\frac{\pi}{2}R}$. The latter is not optimal as it contains a point

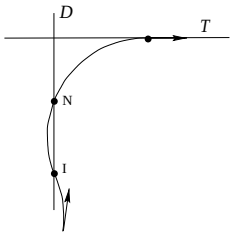

Figure 5: A path $l_a r_b$ with $\frac{\pi}{2}R < b < \frac{3\pi}{2}R$

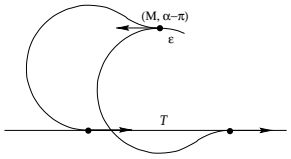

Figure 6: A path $l_{b+\pi R+\varepsilon} r_b$ with $b \in [0, \frac{\pi R}{2}]$

of inflection $I \notin \mathcal{D}$ (see figure 7). It follows that $b = \frac{\pi}{2}R$. On the other hand, if $a = \pi R + \varepsilon$, $\varepsilon > 0$, we can construct an equivalent path $C_\varepsilon C_{\pi R} S C_{\frac{\pi}{2}R}$ which is not optimal as it contains a point of inflection $I \notin \mathcal{D}$ (see figure 8). □

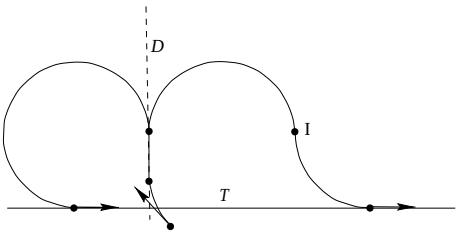

Figure 7: A path $r_a s_d l_b$ with $b = \frac{3\pi}{2}R$

At this stage, gathering the preceding properties we can reduce our search for optimal paths to the family described in table 1.

2.3 Optimal synthesis

We have proven in the previous section that *any* optimal path reaching the directed line must belong to the family in table 1. To solve the optimal control problem this family must be further refined to contain an unique optimal path for linking each point in the state space to $(0, 0)$. To do so, it is be expedient to use path–based coordinates $(s, \tilde{y}, \tilde{\theta}) \in \mathbb{R} \times \mathbb{R} \times S^1$ (see figure 9). Here, s is the abscissa on the path of the normal projection of the center of the vehicle, taken with the same orientation of the path; $\tilde{y}$ represents the (signed) distance from the path of the center of the vehicle, divided by the minimum turning radius R; and $\tilde{\theta} = \theta - \alpha$ is the heading error. The path tracking problem (5) is reformulated in these variables as a minimum–time convergence to the submanifold

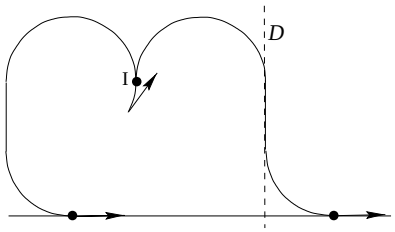

Figure 8: A path $l_a s_d l_{\frac{\pi}{2}R}$ with $a = \pi R + \varepsilon$.

C_a	r_a l_a	$a \in (0, \frac{3\pi}{2}R]$
$C_a C_b$	$l_a r_b$ $r_a l_b$	$b \in (0, \frac{\pi}{2}R]$ and $a \in (0, b + \pi R]$ or $b \in [\pi R, \frac{3\pi}{2}R]$ and $a \in (0, b - \pi R]$
$C_a S_d C_{\frac{\pi}{2}R}$	$r_a s_d r_{\frac{\pi}{2}R}$ $l_a s_d r_{\frac{\pi}{2}R}$ $r_a s_d l_{\frac{\pi}{2}R}$ $l_a s_d l_{\frac{\pi}{2}R}$	$d > 0$ and $a \in [0, \pi R]$

Table 1: Sufficient family of extremal paths connecting to a rectilinear route.

$\mathcal{S} = \left\{(s, \tilde{y}, \tilde{\theta}) : \tilde{y} = 0, \tilde{\theta} = 0\right\}$. Equivalently, we will refer to convergence to $(0,0)$ of the two variables $(\tilde{y}, \tilde{\theta}) \in \mathbb{R} \times S^1$ of the *reduced state space*, which obey the dynamic relationship

$$\begin{array}{rcl} \dot{\tilde{y}} & = & \sin(\tilde{\theta})\, \frac{V}{R} \\ \dot{\tilde{\theta}} & = & \omega \end{array} \tag{13}$$

For each path type contained in the sufficient family we compute, in the reduced space, the domains of possible initial points for paths ending at the origin$(0,0)$.

The construction is done by integrating system (13) backwards for values of ω corresponding to segment types ($\omega = \frac{V}{R}$ for l–arcs, $\omega = -\frac{V}{R}$ for r–arcs, $\omega = 0$ for s–arcs) and for time intervals corresponding to arclengths as specified in table 1. Explicit integration of dynamics (13) gives:

- For $\omega = 0$,

$$\left\{ \begin{array}{ll} \tilde{y}(t) = \tilde{y}(0) + \frac{V}{R}t,\ \tilde{\theta}(t) = +\frac{\pi}{2}, & \text{if } \tilde{y} < -1 \wedge \tilde{\theta} = +\frac{\pi}{2} \\ \tilde{y}(t) = \tilde{y}(0) - \frac{V}{R}t,\ \tilde{\theta}(t) = -\frac{\pi}{2}, & \text{if } \tilde{y} > -1 \wedge \tilde{\theta} = -\frac{\pi}{2} \\ \tilde{y}(t) = 0,\ \tilde{\theta}(t) = 0, & \text{if } \tilde{y} = 0 \wedge \tilde{\theta} = 0 \end{array} \right. \tag{14}$$

- For $\omega = \frac{V}{R}$,

$$\left\{ \begin{array}{l} \tilde{y}(t) = \tilde{y}(0) + \cos(\tilde{\theta}(0)) - \cos(\tilde{\theta}(0) + \frac{V}{R}t), \\ \tilde{\theta}(t) = \tilde{\theta}(0) + \frac{V}{R}t, \end{array} \right. \tag{15}$$

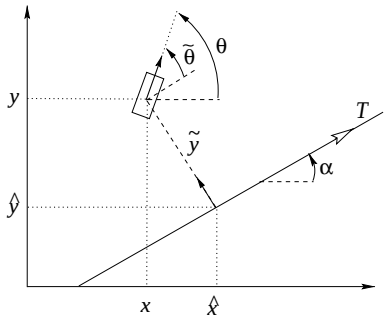

Figure 9: Path–based coordinates.

- For $\omega = -\frac{V}{R}$,

$$\begin{cases} \tilde{y}(t) = \tilde{y}(0) - \cos(\tilde{\theta}(0)) + \cos(\tilde{\theta}(0) - \frac{V}{R}t), \\ \tilde{\theta}(t) = \tilde{\theta}(0) - \frac{V}{R}t, \end{cases} \tag{16}$$

This construction reveals that the mapped domains are adjacents to each other i.e. they just share part of their boundaries. Furthermore, when two different path are defined on the boundary of two adjacent domains, both path have the same length. Hence, an optimal synthesis in the $(\tilde{y}, \tilde{\theta})$ space is derived from table 1 choosing, when more than one solution exists, a particular one to obtain at the end a region which, modulo 2π on $\tilde{\theta}$, covers the whole reduced state space. We obtain a partition of the reduced state space whose cells are described by the table (17).

Path Type	State Space Subset
r	$\{(\tilde{y},\tilde{\theta}) \mid \tilde{\theta} \in (0, \frac{3}{2}\pi), \sigma_R(\tilde{y},\tilde{\theta}) = 0\}$
l	$\{(\tilde{y},\tilde{\theta}) \mid \tilde{\theta} \in (-\frac{3}{2}\pi, 0), \sigma_L(\tilde{y},\tilde{\theta}) = 0\}$
$\mathbf{rl}^{(1)}$	$\{(\tilde{y},\tilde{\theta}) \mid \tilde{\theta} \in [0,\pi), \sigma_R(\tilde{y},\tilde{\theta}) > 0, \sigma_P(\tilde{y},\tilde{\theta}) \leq 0\}$ $\cup\{(\tilde{y},\tilde{\theta}) \mid \tilde{\theta} \in (-\frac{\pi}{2}, 0), \sigma_L(\tilde{y},\tilde{\theta}) > 0, \sigma_P(\tilde{y},\tilde{\theta}) \leq 0\}$ $\cup\{(0,\pi)\}$
$\mathbf{rl}^{(2)}$	$\{(\tilde{y},\tilde{\theta}) \mid \tilde{\theta} \in (-\frac{3}{2}\pi, -\pi], \sigma_P(\tilde{y},\tilde{\theta}) > 0, \sigma_L(\tilde{y},\tilde{\theta}) < 0\}$
$\mathbf{lr}^{(1)}$	$\{(\tilde{y},\tilde{\theta}) \mid \tilde{\theta} \in (0, \frac{\pi}{2}), \sigma_N(\tilde{y},\tilde{\theta}) \geq 0, \sigma_R(\tilde{y},\tilde{\theta}) < 0\}$ $\cup\{(\tilde{y},\tilde{\theta}) \mid \tilde{\theta} \in (-\pi, 0], \sigma_N(\tilde{y},\tilde{\theta}) \geq 0, \sigma_L(\tilde{y},\tilde{\theta}) < 0\}$
$\mathbf{lr}^{(2)}$	$\{(\tilde{y},\tilde{\theta}) \mid \tilde{\theta} \in [\pi, \frac{3}{2}\pi), \sigma_R(\tilde{y},\tilde{\theta}) > 0, \sigma_N(\tilde{y},\tilde{\theta}) < 0\}$
rsr	$\{(\tilde{y},\tilde{\theta}) \mid \tilde{\theta} \in (\frac{\pi}{2}, \frac{3}{2}\pi), \sigma_R(\tilde{y},\tilde{\theta}) < 0\}$
lsr	$\{(\tilde{y},\tilde{\theta}) \mid \tilde{\theta} \in [-\frac{\pi}{2}, \frac{\pi}{2}), \sigma_N(\tilde{y},\tilde{\theta}) < 0\}$
rsl	$\{(\tilde{y},\tilde{\theta}) \mid \tilde{\theta} \in (-\frac{\pi}{2}, \frac{\pi}{2}], \sigma_P(\tilde{y},\tilde{\theta}) > 0\}$
lsl	$\{(\tilde{y},\tilde{\theta}) \mid \tilde{\theta} \in (-\frac{3}{2}\pi, -\frac{\pi}{2}), \sigma_L(\tilde{y},\tilde{\theta}) > 0\}$
sr	$\{(\tilde{y},\tilde{\theta}) \mid \tilde{y} < -1, \tilde{\theta} = \frac{\pi}{2}\}$
sl	$\{(\tilde{y},\tilde{\theta}) \mid \tilde{y} > +1, \tilde{\theta} = -\frac{\pi}{2}\}$
s	$\{(\tilde{y} = 0, \tilde{\theta} = 0)\}$

(17)

where

$$\sigma_R(\tilde{y},\tilde{\theta}) \quad = \quad \tilde{y} + 1 - \cos(\tilde{\theta}), \tag{18}$$

$$\sigma_L(\tilde{y},\tilde{\theta}) = \tilde{y} - 1 + \cos(\tilde{\theta}), \tag{19}$$
$$\sigma_N(\tilde{y},\tilde{\theta}) = \tilde{y} + 1 + \cos(\tilde{\theta}), \tag{20}$$
$$\sigma_P(\tilde{y},\tilde{\theta}) = \tilde{y} - 1 - \cos(\tilde{\theta}). \tag{21}$$

Here, for each path type, arc lengths are as specified in the third column of table 1. Notice that, for notational convenience, each state space subset are denoted by the corresponding path type: when two subsets have the same corresponding path type, we affixed indices to the path type to allow distinction of the two subsets. The synthesis (17) in the reduced state space is described in figure (10). The boundaries between subsets are represented by dotted lines, and the direction of motion is represented by directed curves.

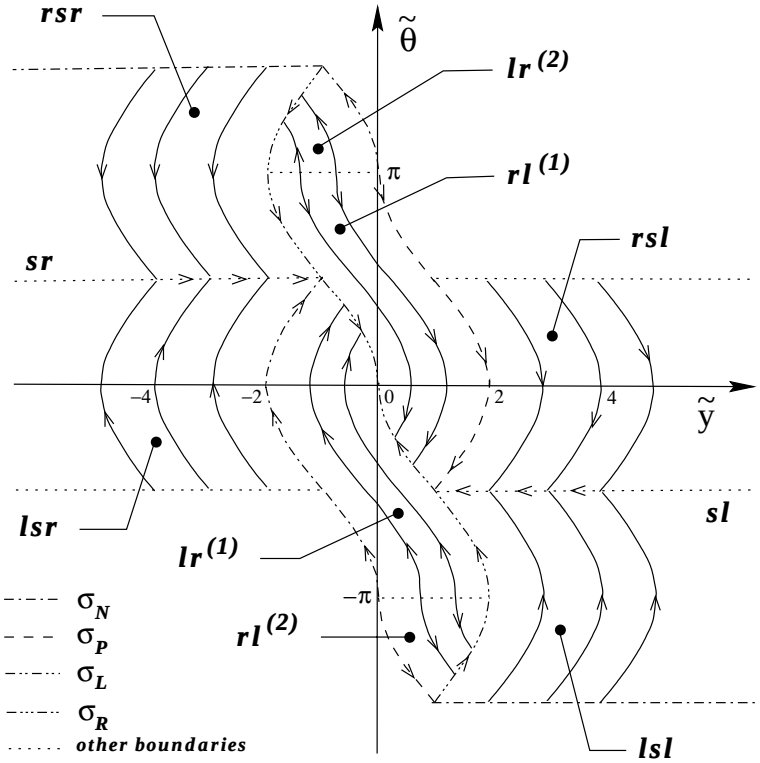

Figure 10: shortest paths synthesis in the $(\tilde{y},\tilde{\theta})$ - plane

By setting $\tilde{y}(t) = \tilde{\theta}(t) = 0$, and solving (15–16), one obtains that the subsets of the reduced state space $\mathbf{r}, \mathbf{l}$ in (17) are connected to the origin by extremal paths of type r and l, respectively, in table 1. Notice that points $(\tilde{y},\tilde{\theta}) = (-1, \frac{3\pi}{2})$ and $(\tilde{y},\tilde{\theta}) = (1, -\frac{3\pi}{2})$, which correspond to arcs $r_{\frac{3\pi}{2}R}$ and $l_{\frac{3\pi}{2}R}$ in table 1, have been excluded from $\mathbf{r}, \mathbf{l}$, as they can be steered to the origin by a different path of the same length.

We proceeded analogously to solve the concatenation of a left and right arc (15–16), and viceversa, so as to obtain that initial points $(\tilde{y}_0,\tilde{\theta}_0)$ in the subsets $\mathbf{rl}^{(1)}, \mathbf{rl}^{(2)}, \mathbf{lr}^{(1)}, \mathbf{lr}^{(2)}$ of (17) that reach the origin by, respectively, rl and lr optimal paths. Solving concatenations of arcs of type rsr, lsr, rsl, and lsl in table 1, for $a > 0$, one gets the corresponding subsets of initial points in the reduced state space $\mathbf{rsr}, \mathbf{lsr}, \mathbf{rsl}, \mathbf{lsl}$ in (17). In the particular case that $a = 0$, concatenations of arcs of type sr and sl must be solved, yielding initial points $(\tilde{y}_0,\tilde{\theta}_0)$ in the subsets $\mathbf{sr}, \mathbf{sl}$ of (17), respectively. Finally, solving arcs of type s backward from the origin one obtains the origin of the reduced state space $\mathbf{s} = \{(0,0)\}$.

Therefore, as this partition defines a unique optimal path for linking each point to the origin, the optimal control problem is completely solved. We have the following proposition:

Proposition 1 *The twelve subsets* $\mathbf{l}$, $\mathbf{r}$, $\mathbf{rl}^{(1)}$, $\mathbf{lr}^{(1)}$, $\mathbf{rl}^{(2)}$, $\mathbf{rl}^{(2)}$, $\mathbf{rsr}$, $\mathbf{lsr}$, $\mathbf{rsl}$, $\mathbf{lsl}$, $\mathbf{sr}$, $\mathbf{sl}$, *plus the origin* $\tilde{\mathbf{o}} = \{(0,0)\}$ *determine a partition of the reduced state space, (modulo* 2π *on* $\tilde{\theta}$*) defining a synthesis of optimal paths.*

2.4 Regularity of the synthesis

The optimality of the synthesis can be confirmed a posteriori by using a verification theorem based on the notion of regular synthesis [14]. We consider the the classification of optimal feedbacks provided by Bressan and Piccoli [3]. This result provides sufficient optimality conditions under the hypotheses that the synthesis verifies some regularity conditions. Consider the construction defined by (17). Every trajectory defined by the synthesis is extremal as it verifies the necessary conditions of PMP. Furtheremore, the synthesis is total as the thirteen subsets $\mathbf{l}$, $\mathbf{r}$, $\mathbf{rl}^{(1)}$, $\mathbf{lr}^{(1)}$, $\mathbf{rl}^{(2)}$, $\mathbf{rl}^{(2)}$, $\mathbf{rsr}$, $\mathbf{lsr}$, $\mathbf{rsl}$, $\mathbf{lsl}$, $\mathbf{sr}$, $\mathbf{sl}$ and $\mathbf{s}$ have void mutual intersections, and their union corresponds to the whole reduced state space $\mathbb{R} \times S^1$. Moreover, the cost function of our optimal control problem, namely the length, is continuous and the synthesis function is differentiable almost everywhere (as it is piecewise constant and takes its values in $\{-1, 0, +1\}$). Hence, the synthesis verifies the required regularity conditions and the optimality of paths follows.

3 Optimal feedback control

In this section, we consider the stability and convergence properties of a feedback control law $\omega(\tilde{y}, \tilde{\theta})$ that is piecewise constant over the thirteen non–overlapping regions of the synthesis (17). Switchings of the control signal will occur as the continuous evolution of the system state leaves a subset of the partition and enters a different one. Due to such coupling of continuous and discrete phenomena, a proper framework to describe and study the resulting closed–loop system is the hybrid systems framework (see e.g. [12]).

The hybrid optimal feedback control is characterized by three modes:

$$\begin{aligned} &\bullet \quad \textit{go\_straight}, \quad \text{where } \omega = 0; \\ &\bullet \quad \textit{turn\_right}, \quad \text{where } \omega = -\frac{V}{R}; \\ &\bullet \quad \textit{turn\_left}, \quad \text{where } \omega = +\frac{V}{R}. \end{aligned} \tag{22}$$

selected, according to Proposition 1, as follows

$$\begin{aligned} &\bullet \ \textit{go\_straight}, \\ &\quad \text{if } (\tilde{y}, \tilde{\theta}) \in \Omega^0 = \mathbf{sr} \cup \mathbf{sl} \cup \mathbf{s}; \\ &\bullet \ \textit{turn\_right}, \\ &\quad \text{if } (\tilde{y}, \tilde{\theta}) \in \Omega^- = \mathbf{r} \cup \mathbf{rsr} \cup \mathbf{rsl} \cup \mathbf{rl}^{(1)} \cup \mathbf{rl}^{(2)}; \\ &\bullet \ \textit{turn\_left}, \\ &\quad \text{if } (\tilde{y}, \tilde{\theta}) \in \Omega^+ = \mathbf{l} \cup \mathbf{lsr} \cup \mathbf{lsl} \cup \mathbf{lr}^{(1)} \cup \mathbf{lr}^{(2)}; \end{aligned} \tag{23}$$

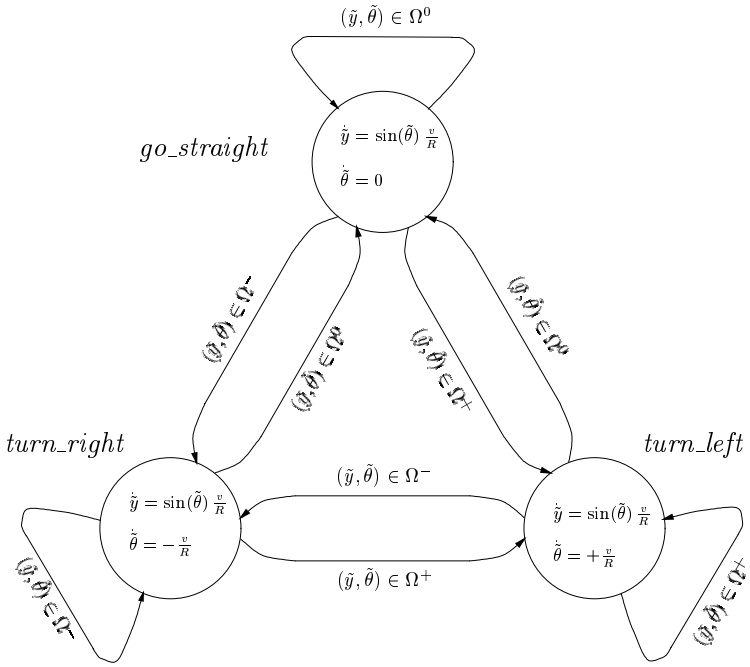

Figure 11: Hybrid model of the closed-loop system.

In figure 11 the model of the closed–loop hybrid system obtained applying feedback control (22–23) to dynamics (13) is reported using the hybrid automaton formalism (see [13]). The semantic of the closed–loop hybrid model is very simple: the hybrid system remains in a given mode $q \in \{go\_straight, turn\_left, turn\_right\}$ as long as all the guard conditions $(\tilde{y},\tilde{\theta}) \in \Omega$ located on the outgoing arcs are false; when one of them becomes true, the hybrid system switches to the corresponding new mode. For, by construction, sets Ω^0,Ω^+ and Ω^- are a partition of the domain $\mathcal{D}_{(\tilde{y},\tilde{\theta})}$, the hybrid automaton is deterministic.

We have thus far established that the discontinuous control law control (22–23) is an optimal feedback for system (13). It should be noticed that optimality of feedback does not imply Lyapunov stability: for instance, the synthesis of Dubins' paths for a vehicle (3) to reach a fixed configuration, does not yield a stabilizing law (such system is not small time locally controllable). However, in our case, the following applies.

Proposition 2 *System (13) under feedback control (22–23), is globally asymptotically stable.*

Proof: The proof of convergence is implied by the previous discussion (actually, a stronger statement is true, that the equilibrium configuration is reached in finite time). The proof of stability is based on a direct application of Lyapunov's definition in the reduced space of configurations $\xi \stackrel{def}{=} (\tilde{y},\tilde{\theta})^T$

$$\forall \epsilon, \exists \delta : \|\xi_0\| < \delta \Rightarrow \|\phi_{\xi_0}(t)\| < \epsilon, \forall t, \tag{24}$$

where $\phi_{\xi_0}(t)$ is the solution of (13) with $\xi(0) = \xi_0$ at time t.

Let $W(\xi) = \tilde{y}^2 + \tilde{\theta}^2$, and consider its derivatives along the trajectories of the system $\dot{W} = \frac{2V}{R}\tilde{y}\sin\tilde{\theta} +$

$\tilde{\theta}\omega$. In particular, in the unit disk $W(\xi) < 1$, by applying the control (22–23), we have

$$\dot{W}(\tilde{y},\tilde{\theta}) = \begin{cases} (\tilde{y}|\sin(\tilde{\theta})| - |\tilde{\theta}|)\frac{2V}{R} < 0, \\ \quad \Big[(\tilde{y},\tilde{\theta}) \in \mathbf{rl}^{(1)} \wedge \tilde{\theta} > 0\Big] \vee (\tilde{y},\tilde{\theta}) \in \mathbf{r} \\ (-\tilde{y}|\sin(\tilde{\theta})| + |\tilde{\theta}|)\frac{2V}{R} \geq 0, \\ \quad (\tilde{y},\tilde{\theta}) \in \mathbf{rl}^{(1)} \wedge \tilde{\theta} \leq 0 \\ (-\tilde{y}|\sin(\tilde{\theta})| - |\tilde{\theta}|)\frac{2V}{R} < 0, \\ \quad \Big[(\tilde{y},\tilde{\theta}) \in \mathbf{lr}^{(1)} \wedge \tilde{\theta} < 0\Big] \vee (\tilde{y},\tilde{\theta}) \in \mathbf{l} \\ (\tilde{y}|\sin(\tilde{\theta})| + |\tilde{\theta}|)\frac{2V}{R} \geq 0, \\ \quad (\tilde{y},\tilde{\theta}) \in \mathbf{lr}^{(1)} \wedge \tilde{\theta} \geq 0 \end{cases} \tag{25}$$

Integrating (25) for any $\beta < \frac{1}{2}$, we obtain

$$\begin{aligned} &\sup_{\|\xi_0\| \leq \beta} \sup_{t \in \mathbb{R}^+} W(\phi_{\xi_0}(t)) = \sup_{t \in \mathbb{R}^+} W(\phi_{(\pm\beta,0)}(t)) \\ &= \frac{\beta^2}{4} + \arccos^2(1 - \frac{\beta}{2}) = \bar{W}(\beta) < 1 \end{aligned}$$

Hence, $\forall \epsilon > 0$, choosing either $\delta = \frac{1}{2}$ if $\epsilon \geq [\bar{W}(\frac{1}{2})]^{\frac{1}{2}}$, or $\delta = \bar{W}^{-1}(\epsilon^2)$ otherwise, for any ξ_0 with $\|\xi_0\| < \delta$ we obtain $\|\phi_{\xi_0}(t))\| < \epsilon < 1$. □

4 Experimental results

To check the practical feasibility of the feedback control strategy above illustrated, experimental tests have been conducted with a wheeled vehicle (TRC's "Labmate"). The vehicle does not have an inherent limitation on its turning radius: however, to practical purposes, too high curvatures should be avoided not to introduce significant nonlinearities in the system (due to slippage of the wheels). We chose to set the minimum turning radius to 25 cm. in our experiments, and set the forward velocity to 5 cm/sec. Information on the vehicle position and orientation is obtained by processing odometric information (encoder measurement of wheel rotations) along with angular measurements given by a ladar sensor (Siman's "Robosense") mounted on the vehicle. Computations are performed on a remote PC, linked to an on–board processor through a radio modem link. In order to simulate a situation where computational resources for the control system are shared with other processes, and are scarce, we set the sampling frequency to a low 10 Hz.

The main causes of non–ideality of the experimental setup, w.r.t. to the model used in the theoretical development above are thus three: i) the vehicle possesses nonnegligible dynamics; ii) state measurements are affected by errors, and iii) low sampling time.

Implementations of switching control signals such as that proposed in (23), on physical plants with such nonidealities, are doomed to produce vibratory phenomena known as "chattering". An example of this behaviour is reported in figure 12, referring to an experiment where raw data from the ladar sensor where fed directly to the control law (23). The optimal connecting path is in this case of type **rl**, but its execution is rather imprecise.

The chattering problem has been extensively studied in relation to sliding–mode control (see e.g. [25, 20]), and solutions have been proposed that modify abrupt steps in the control with a saturation–like effect. The effect of such smoothing of the control is to introduce a thin "boundary layer" around the curves in state space where discontinuity of the control arises, wherein the system dynamics

behave differently from what expected with perfect switching control. As a net effect on the global performance, we have that asymptotic stability claims reduce to uniform ultimate boundedness of trajectories. The claim of optimality of trajectories also fails in this case, but a reasonably good approximation of the optimum can be obtained, as shown in the experimental results below. A detailed analysis of the behaviour of the proposed technique with boundary layers is currently under investigation, but goes beyond the scope of this paper. Furthermore, a refinement of localization accuracy can be obtained by proper fusion of the two information sources (odometry and triangulation) in an extended Kalman filter algorithm.

Results of a typical experiment with boundary layer and filtered measurements are reported in figures 12 and 13. In this case, the shortest connecting path to the rectilinear route is of **lsr** type.

5 Conclusions

We presented a feedback control technique for connecting the kinematic model of unidirectional nonholonomic vehicles to rectilinear routes. The proposed solution, besides being of practical relevance to many application domains (automated vehicles, aircraft cruise control), has the interesting theoretical property of being an optimal, globally asymptotic stabilizing law for a nontrivial system. We reported on an experimental implementation of the technique, which exhibits some problems related to nonidealities of the physical plant. However, these problems can be overcome by application of suitable smoothing and filtering techniques, as documented by experimental validation.

Our results could be extended in several directions. The feedback control law can be applied to following more general routes, provided that the route curvature is moderate and continuous, by applying it to the tangent line to the route at the point instantaneously closest to the vehicle position. More generally, the optimality of the synthesis seems to indicate some degree of robustness of the proposed controller with respect to modeling errors and measurement noise: these aspects however should be studied further. Current work is being devoted to investigation of such extensions.

References

[1] M. Aicardi, G. Casalino, A. Bicchi and A. Balestrino: "Closed Loop Steering of Unicycle–like Vehicles via Lyapunov Techniques", IEEE Robotics and Automation Magazine, pp. 27–35, March 1995.

[2] A. Astolfi: "Exponential Stabilization of a Car–like Vehicle", in Proc. 1995 IEEE International Conference on Robotics and Automation, pp. 1391–1396, 1995.

[3] A. Bressan and B. Piccoli, "A generic classification of time optimal planar stabilizing feedbacks", SIAM Journal on Control and Optimization 36, (1998), pp.12–32.

[4] J.D. Boissonnat, A. Cerezo and J. Leblong, "Shortest paths of bounded curvature in the plane," in *IEEE Int. Conf. on Robotics and Automation*, Nice, France, 1992.

[5] R.W. Brockett: "Asymptotic Stability and Feedback Stabilization", in Differential Geometric Control Theory, Brockett, Millmann and Sussmann, eds., pp. 181–191, Boston, U.S., 1983.

[6] X-N. Bui, P. Souères, J-D. Boissonnat, and J-P. Laumond, "The shortest paths synthesis for nonholonomic robots moving forwards," *Proc. of the IEEE Int. conf. on Robotics and Automation, San Diego, California, USA, 1993.*

[7] R.T. M'Closkey and R.M. Murray: "Exponential Stabilization of Driftless Nonlinear Control Systems via Time–Varying, Homogeneous Feedback", 33rd IEEE Conference on Decision and Control, 1994.

[8] B. d'Andréa–Novel, G. Bastin and G. Campion: "Dynamic Feedback Linearization of Nonholonomic Wheeled Mobile Robots", in Proc. 1992 IEEE International Conference on Robotics and Automation, pp. 2527–2532, Nice, France, 1992.

[9] A. De Luca and M.D. Di Benedetto: "Control of Nonholonomic Systems via Dynamic Compensation", Kybernetika, vol. 29, no. 6, pp. 593–608, 1993.

[10] L. E. Dubins: "On curves of minimal length with a constraint on average curvature and with prescribed initial and terminal positions and tangents", American Journal of Mathematics, vol.79, pp.497–516, 1957.

[11] J. Guldner and V.I. Utkin: "Sliding Mode Control of Mobile Robots", in Proc. IEEE Workshop on Robust Control via Variable Structure and Lyapunov Techniques, pp. 4–11, Benevento, Italy, 1994.

[12] T. A. Henzinger and S. S. Sastry (eds.), *HSCC98, Hybrid Systems: Computation and Control*, vol. 1386 of *Lecture Notes in Computer Science*, Springer, 1998.

[13] T. A. Henzinger, *The theory of hybrid automata*, in Proc. 11th Annual Symposioum on Logic in Computer Science, pp. 278–292, IEEE Computer Society Press, 1996.

[14] B. Piccoli and H. J. Sussmann, *Regular Synthesis and Sufficiency Conditions for Optimality*, SISSA-ISAS (Int. School of Advanced Studies), Trieste, Italy, 1998.

[15] L.S Pontryagin, V.G. Boltianskii, R.V. Gamkrelidze, and E.F. Mishenko. "The mathematical Theory of Optimal Processes," *Interscience Publishers,* 1962.

[16] J. A. Reeds, R. A. Shepp: "Optimal Paths for a Car that Goes both Forward and Backward", Pacific Journal of Mathematics, vol. 145(2), 1990.

[17] M. Sampei, T. Tamura, T. Kobayashi and N. Shibui: "Arbitray Path Tracking Control of Articulated Vehicles Using Nonlinear Control Theory", IEEE Transactions on Control Systems Technology, vol. 3, no. 1, pp. 125–131, 1995.

[18] C. Samson: "Control of Chained Systems Application to Path Following and Time–Varying Point–Stabilization of Mobile Robots", IEEE Transactions on Automatic Control, vol. 40, no. 1, pp. 64–77, 1995.

[19] N. Sarkar, X. Yun and V. Kumar: "Control of Mechanical Systems with Rolling Constraints: Application to Dynamic Control of Mobile Robots", International Journal of Robotics Research, vol. 13, no. 1, pp. 55–69, 1994.

[20] J.J.E Slotine, and S. S. Sastry: "Tracking control of nonlinear systems using sliding surfaces with applications to robot manipulators", Int. J. Control, vol 38, pp.465–492, 1983.

[21] O.J. Sordalen and C. Canudas de Wit: "Exponential Control Law for a Mobile Robot: Extension to Path Following", IEEE Transactions on Robotics and Automation, vol. 9, no. 6, pp. 837–842, 1993.

[22] O.J. Sordalen and O. Egeland: "Exponential Stabilization of Nonholonomic Chained Systems", IEEE Transactions on Automatic Control, vol. 40, no. 1, pp. 35–49, 1995.

[23] P. Souères, J-P. Laumond "Shortest Paths Synthesis for a Car-Like Robot," *IEEE Transaction on Automatic Control, Vol. 41, NO. 5, May 1996.*

[24] H.J. Sussmann and W. Tang, "Shortest paths for the Reeds-Shepp car : a worked out example of the use of geometric techniques in nonlinear optimal control," Report SYCON-91-10, Rutgers University, 1991.

[25] Utkin, V.I.: "Sliding Modes and their Application in Variable Structure Systems", Mir Publishers, Moscov, 1978.

[26] G. Walsh, D. Tilbury, S. Sastry, R. Murray and J.P. Laumond: "Stabilization of Trajectories for Systems with Nonholonomic Constraints", memorandum no. UCB/ERL M92/11, Electronics Research Laboratory, College of Engineering, University of California, Berkeley, U.S., 28 January 1992.

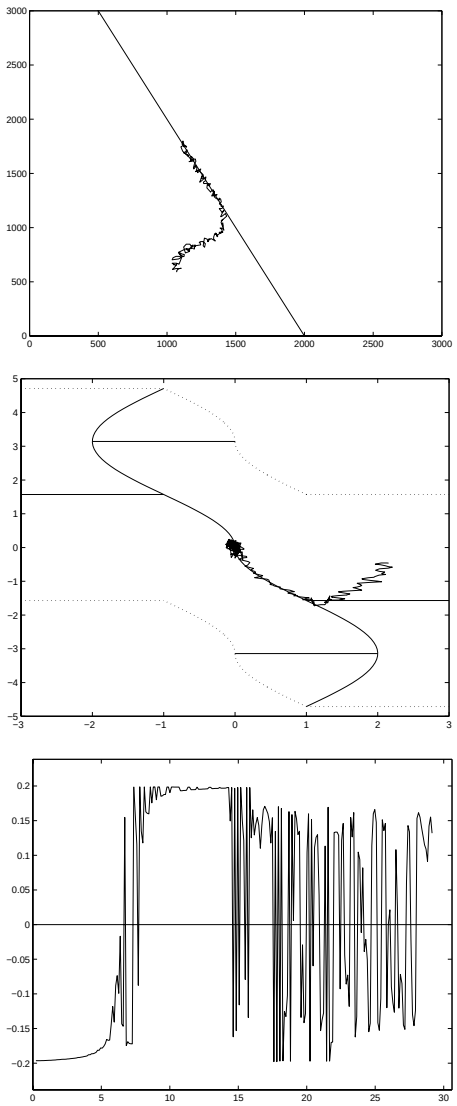

Figure 12: *Experiment 1: (Chattering control) From top to down: reference route and vehicle position as measured during execution of the feedback control law; the same positional data in the reduced state space; control input vs. time.*

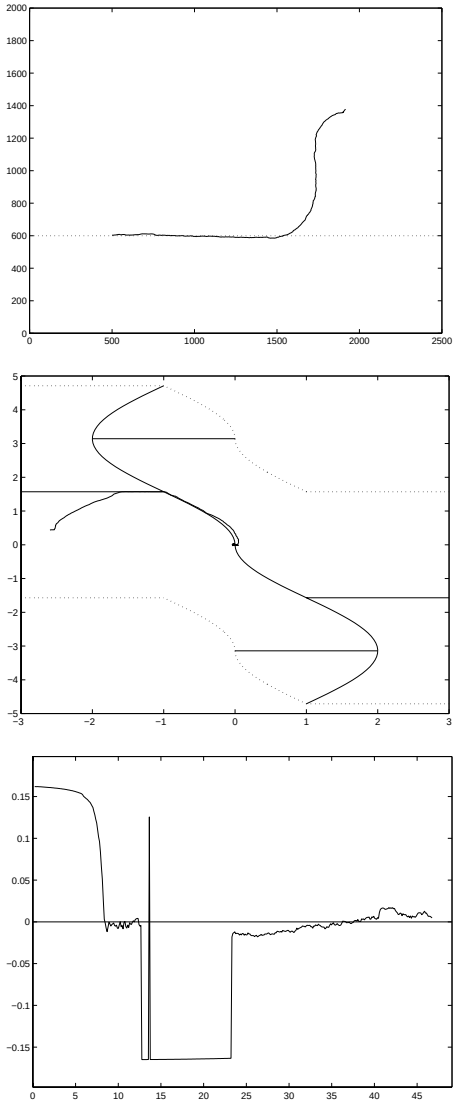

Figure 13: *Experiment 2: Same sequence as before with smoothed control.*